Nordic Hydrology 3, 1972, 22–43
Published by Munksgaard, Copenhagen, Denmark

POLE-TO-POLE WATER BALANCE FOR THE IGY FROM AEROLOGICAL DATA

JOSE P. PEIXOTO

Massachusetts Institute of Technology, Cambridge, Massachusetts,
and the University of Lisbon

The present study gives a discussion of the water balance on a planetary scale during the IGY covering the mean and the seasonal conditions for the calendar year 1958. The study includes analyses of the amount of precipitable water, of the vertically integrated transport vector field and of the divergence of water vapor flux for all the globe. Some implications of the water vapor distribution in the atmosphere, its transport, and divergence fields are deduced which bear some importance for hydrology. The water balance based upon the various water vapor fields is examined and the inferred values obtained from the analysis of the water vapor divergence field are compared with estimates of evaporation and precipitation obtained from independent climatological sources.

This study must be considered within the framework of previous work performed by the writer and his associates published elsewhere. Daily values of the wind field and specific humidity fields for each individual station at four pressure levels (1000, 850, 700, 500 and in some cases, 300 mb) in the atmosphere were used for the analysis. An extensive coverage of about 450 stations formed the network, and where the choice was possible, the most reliable stations were selected. Although the network is not yet sufficiently dense over large oceanic areas of the Southern Hemisphere and over the central part of South America, it appears that the IGY data are the best yet available on a planetary scale for undertaking the global study of the water vapor fields in the atmosphere on a global basis. Annual and seasonal means were then computed and the results integrated vertically to obtain precipitable water, the total vector transport field, and finally the divergence field using the finite difference method. The seasons considered in the present study are the two semester seasons: April–September and January–March, October–December (composite winter).

MEAN STORAGE OF THE ATMOSPHERE

The formulation principles of the problem and the procedures followed are those already described on various occasions by the writer (see, e.g., Peixoto 1970a). The spatial distributions of the mean storage in the atmosphere for both semesters of precipitable water, $\overline{W}(\lambda, \Phi)$ are presented in Figs. 1 and 2. Here λ is longitude and Φ is latitude. The precipitable mean water is expressed by $W \equiv \frac{1}{g}\int_{p}^{p_o} q\,dp$, where g is the acceleration of gravity, q the specific humidity and p the pressure. The bar operator indicates a time average of the specified quantity for the time interval τ

$$\overline{(\ )} = \frac{1}{\tau}\int_{\tau} (\ )\,dt$$

The dots in the charts indicate the distribution of the stations used in the present investigation. The chart with the mean annual distribution is not shown here since it was presented and discussed by the writer elsewhere (Peixoto 1970a).

The distribution of precipitable water in both semesters shows a general increase at all the latitudes of moisture content from the corresponding cold season to the warm season, which is clearly seen from the inspection of the isolines of 1 gm cm^{-2} and 3 gm cm^{-2}, for instance, in either hemisphere, in both maps. In any case, the distribution is more regular over the Southern Hemisphere, where 80.9 % of the surface is covered by the oceans and the topography is considerably different from that of the Northern Hemisphere. We may see that the physiography of the globe influences the distribution of the water vapor storage, altering the quasi-zonally symmetric regime that would be expected according to the mean distribution of temperature in the lower layers of the atmosphere, with a maximum over the equatorial zone and decreasing monotonically towards the poles. The equatorial zone shows various centers of maxima exceeding 5.5 gm cm^{-2} in some cases. This belt of maxima is slightly displaced southward of the equator in the Oct.–March semester chart

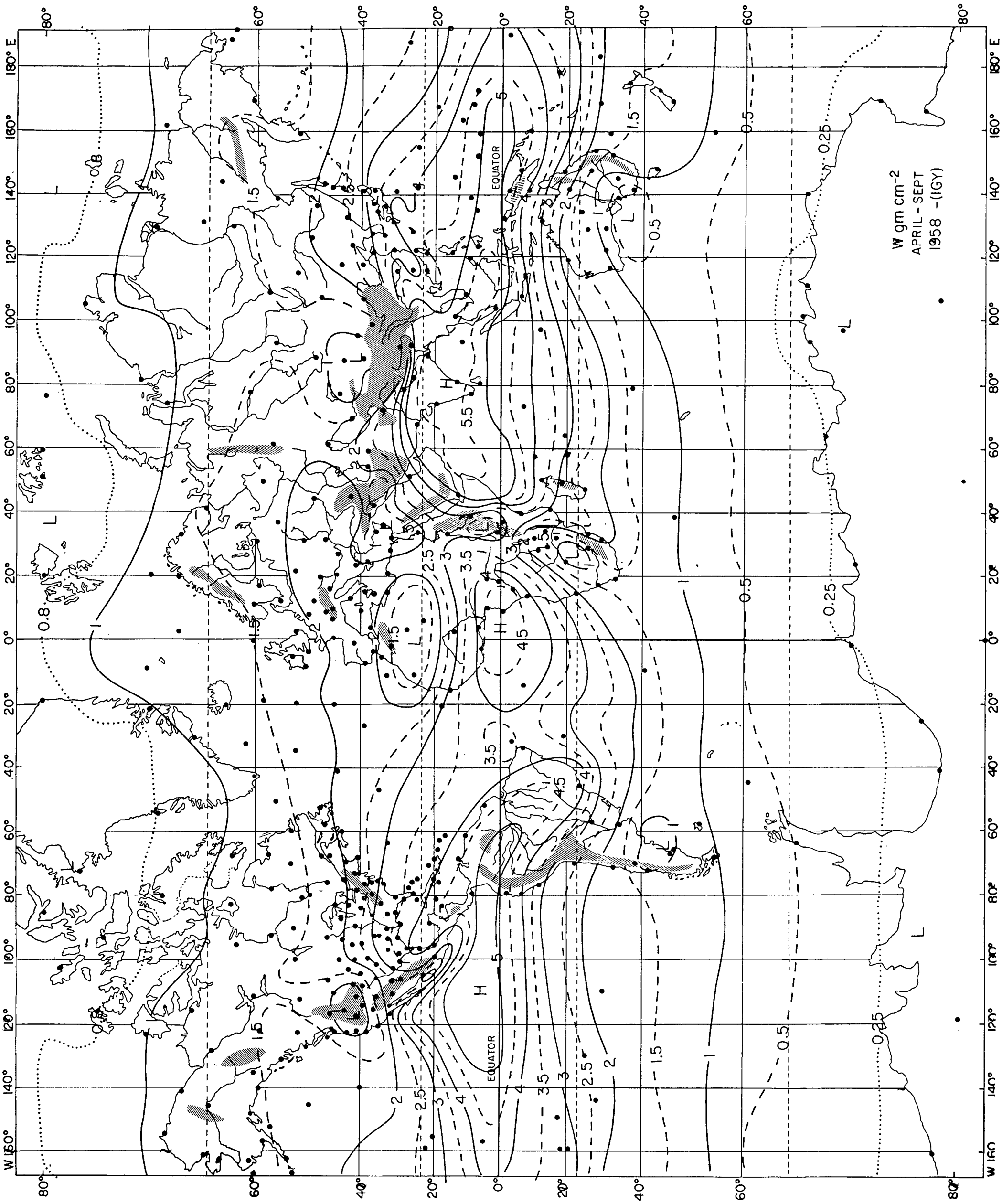

Fig. 1.
Distribution of the two-dimensional mean moisture content field of the atmosphere, $\overline{W}(\lambda, \Phi)$ in gm per cm² for the IGY April–September semester. Isoline spacing (full curves) 1 gm cm⁻².

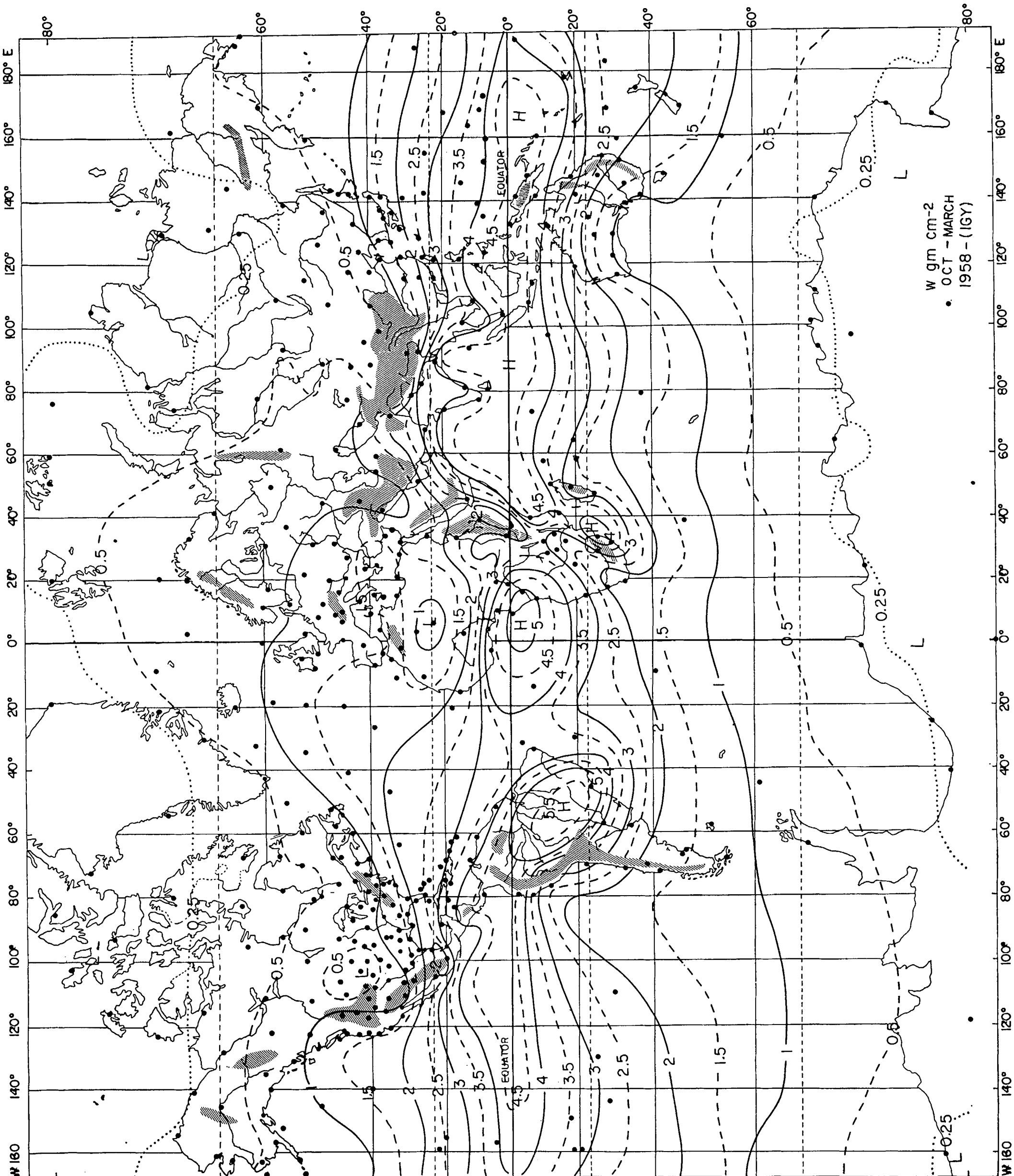

Fig. 2.
Distribution of the two-dimensional mean moisture content field of the atmosphere, $\overline{W}(\lambda,\Phi)$ in gm per cm^2 for the IGY October–March semester, Isoline spacing (full curves) 1 gm cm^{-2}.

which corresponds to the warm season of the Southern Hemisphere. However, the maximum value is still observed over the Amazonian Basin. The actual maps agree remarkably well with the corresponding analysis for the African continent obtained by Peixoto and Obasi (1965) and the Australian as presented by Hutchings (1961). The connection between the centers of minima and the arid and semi-arid regions is also apparent. As expected, over the polar regions the values are very low. Furthermore, the effects of topography are also evident over the Himalayan Mountains, over the highlands of Ethiopia and the mountains of Kenya, and over the Andes. Over the Southern Hemisphere the isolines of water vapor content run generally along latitude circles with departures from this idealized zonal distribution induced by the presence of the South American continent, by Africa and by Australia. The distortion is more pronounced during the "warm season".

In Table 1 the mean annual and mean seasonal values of the zonally averaged precipitable water $[\overline{W}]$ for various latitudes are given. Here the brackets [ ] represent the mean zonal operator defined by $[(\ )] = \frac{1}{2\pi} \varphi (\ )\, d\lambda$. These values are also shown in Fig. 3. They summarize the global distribution of $[\overline{W}]$ on a planetary scale, thus giving an idea of the general characteristics and strength of the "gaseous hydrosphere" of the earth, to use Starr's expression. In order to improve the picture of its structure, vertical meridional cross sections through the atmosphere showing the latitudinal distribution of the mean zonal specific humidity $[\overline{q}]$ for yearly and seasonal conditions, as well as some vertical soundings of the mean specific humidity for various latitudes, are presented in Fig. 4 and 5 respectively.

The highest mean moisture storage occurs in the equatorial regions and decreases very rapidly poleward with a steep gradient in the subtropical latitudes. As the figures show, the seasonal changes of the mean storage, $\triangle\, [\overline{W}]$, over the year are very small indeed. Over the Northern Hemisphere the change in storage between summer and winter is about 0.80 gm cm^{-2}, whereas in the Southern Hemisphere it is only around 0.24 gm cm^{-2}. The overall moisture storage for the whole earth is of the order of 2.57 gm cm^{-2} which amounts approximately to a total of 1.3×10^{16} kg of water in the mean. This quantity is of the same order of magnitude as the mass of the water contained in all the lakes amounting approximately to 6.5×10^{16} kg. The amount of water flowing in the rivers can be estimated at any single moment to be about 10^{15} kg.

Fig. 4 shows the vertical distribution of the mean moisture (specific humidity) over various latitudes considered to be the most representative. The mean specific humidity $[\overline{q}]$ decreases rapidly with height with a strong gradient in the lowest layers of the atmosphere following almost an exponential law. The

Table 1.

Distribution of zonally averaged moisture content $[\overline{W}]$ for yearly and semester conditions in gm cm^{-2} from aerological data during the IGY.

Deg. Lat.	0	5	10	15	20	25	30	35	40	45	50	55	60	65	70	75	80
Northern Hemisphere																	
Year	4.39	4.31	3.99	3.63	3.11	2.78	2.18	1.83	1.64	1.47	1.32	1.19	1.04	0.89	0.70	0.58	0.48
Apr.–Sept.	4.41	4.55	4.42	4.03	3.56	3.25	2.64	2.24	2.02	1.84	1.70	1.57	1.40	1.23	0.97	0.82	0.72
Oct.–Mar.	4.38	4.10	3.62	3.22	2.73	2.30	1.72	1.39	1.15	0.96	0.81	0.72	0.55	0.43	0.29	0.24	0.19
Southern Hemisphere																	
Year	4.39	4.27	4.05	3.64	3.16	2.63	2.17	1.84	1.61	1.41	1.21	0.96	0.72	0.52	0.30	0.20	0.10
Apr.–Sept.	4.41	4.15	3.77	3.26	2.77	2.32	1.90	1.57	1.36	1.19	1.01	0.76	0.83	0.36	0.25	0.14	0.07
Oct.–Mar.	4.38	4.38	4.09	3.70	3.32	2.87	2.43	2.07	1.77	1.50	1.23	1.12	0.74	0.54	0.38	0.24	0.14

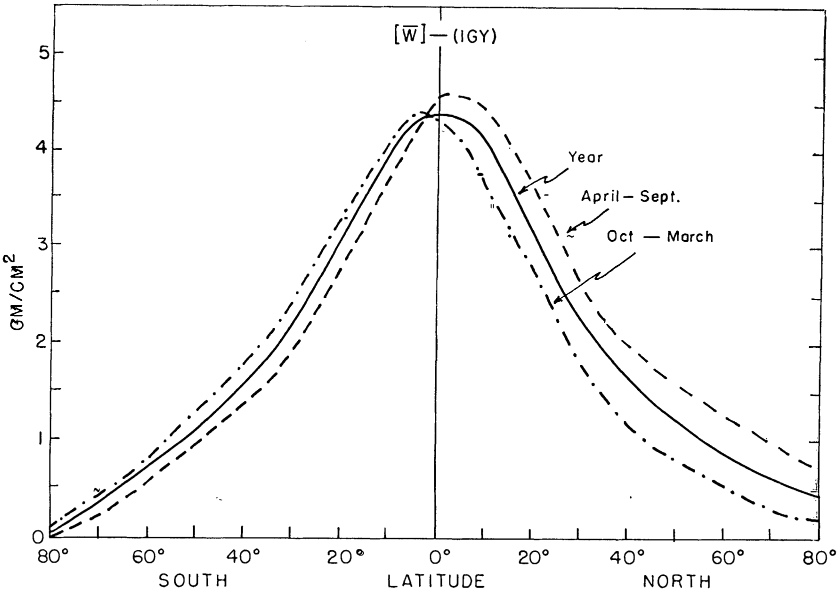

Fig. 3.

Meridional profile of the mean zonal water vapor content $[\overline{W}(\Phi)]$ for the IGY yearly and seasonal mean conditions computed from atmospheric data in units of gm cm^{-2}.

existence of a strong gradient of specific humidity in the lower layers is to be expected from the intense transfer of water vapor from the surface to the atmosphere coupled with its transport aloft by convection and turbulence. More than 50 % of the storage is confined to the layer between the ground and 850 mb (15 % of the total mass of the atmosphere) and more than 90 % in the lower half on the atmosphere. The largest variability of q, as shown by the values of the mean standard deviation $\sigma(q)$ not shown in the present study, occurs, however, in subtropical and midlatitude zones in the layer between the ground and the 850 mb level. It is interesting to note in Figs. 4 and 5 the reversal of the mean conditions over both hemispheres where the semester distributions are taken "in toto" as compared with a quasi-symmetry when one considers the hemispheric "cold and warm seasons".

THE AREAL RUN-OFF

A chart, showing the planetary distribution of the total mean horizontal vector transfer $\overline{\vec{Q}}(\lambda,\Phi)$ of water vapor (areal run-off) for the yearly mean conditions, so that

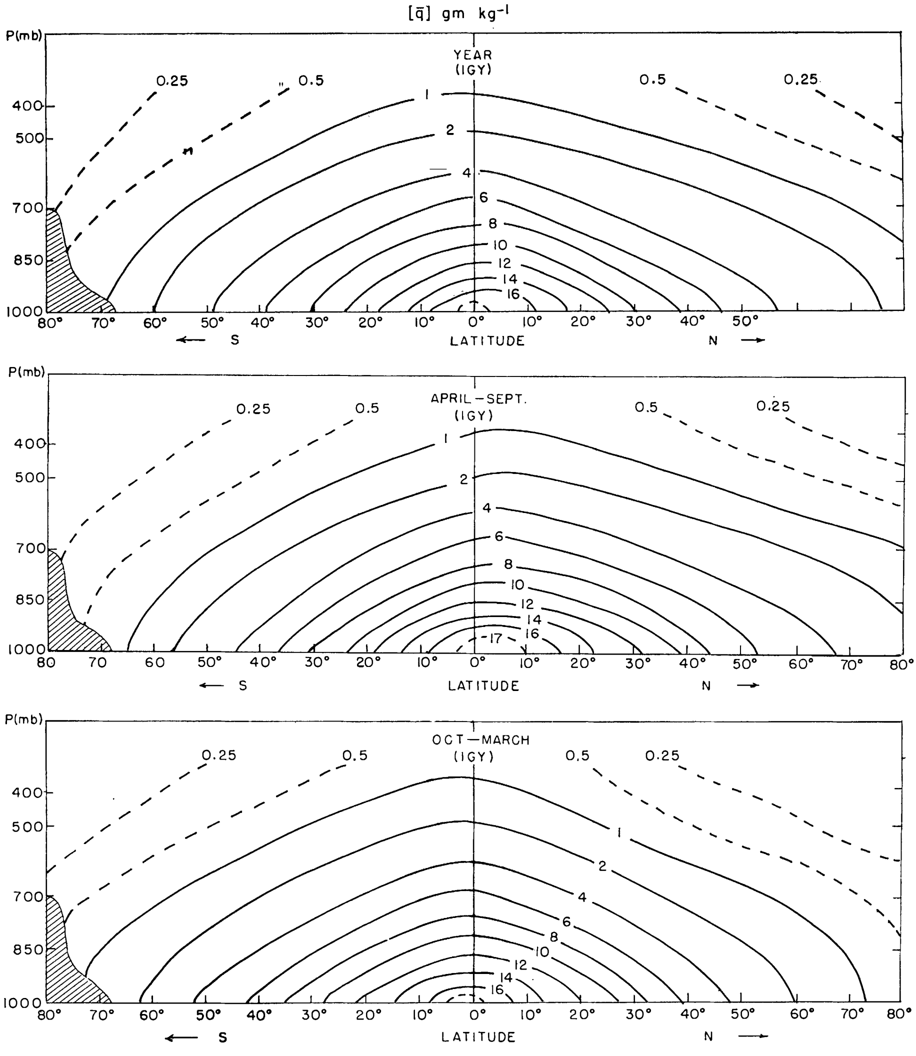

Fig. 4.

Vertical meridional cross sections through the atmosphere showing the distribution of the mean zonal specific humidity $[\bar{q}]$ for the IGY yearly and seasonal conditions. The units are gm kg-1.

$$\overline{\vec{Q}}(\lambda,\Phi) = \overline{Q_\lambda \vec{i_\lambda}} + \overline{Q_\Phi \vec{i_\Phi}}$$

is shown in Fig. 6. Here $\overline{Q}_\lambda$ and $\overline{Q}_\Phi$ are the horizontal components of $\overline{\vec{Q}}$ in the λ and Φ directions. They are given respectively by

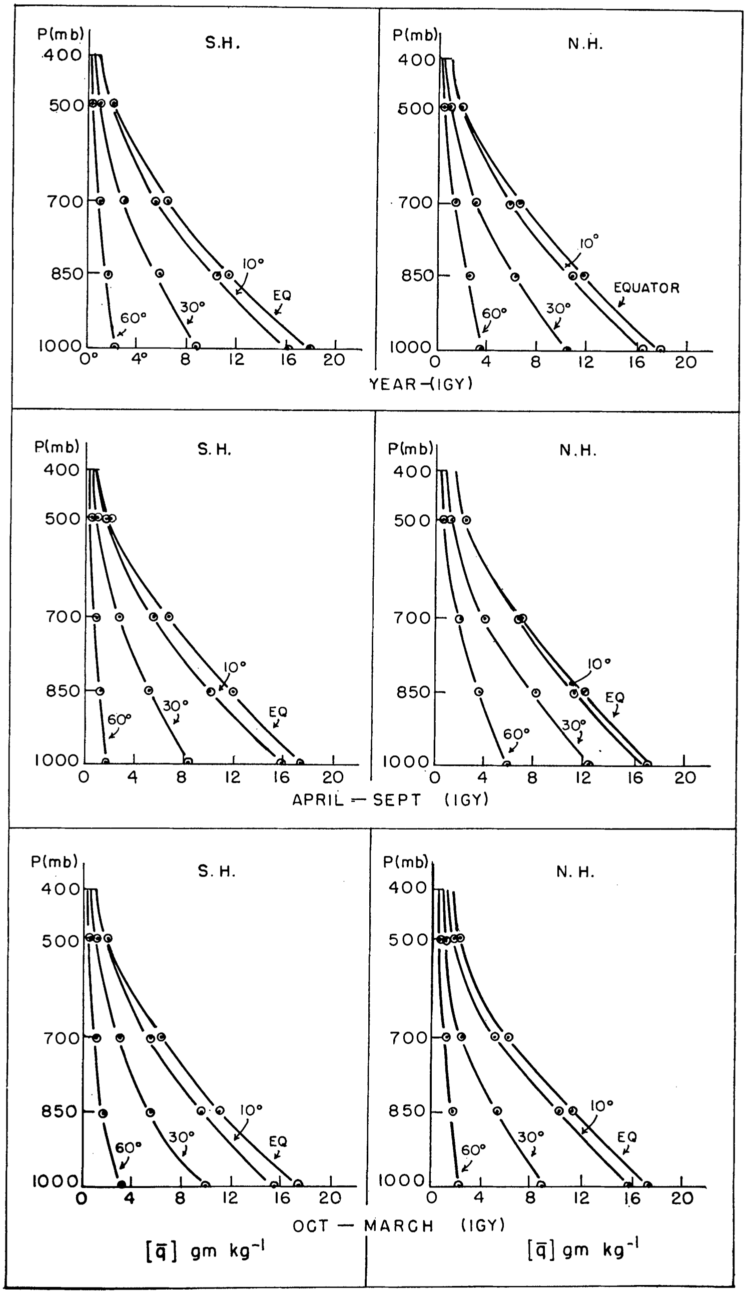

Fig. 5.

Vertical distribution of the mean zonal specific humidity $[\bar{q}]$ at various latitudes in gm kg-1 for the IGY yearly and seasonal conditions.

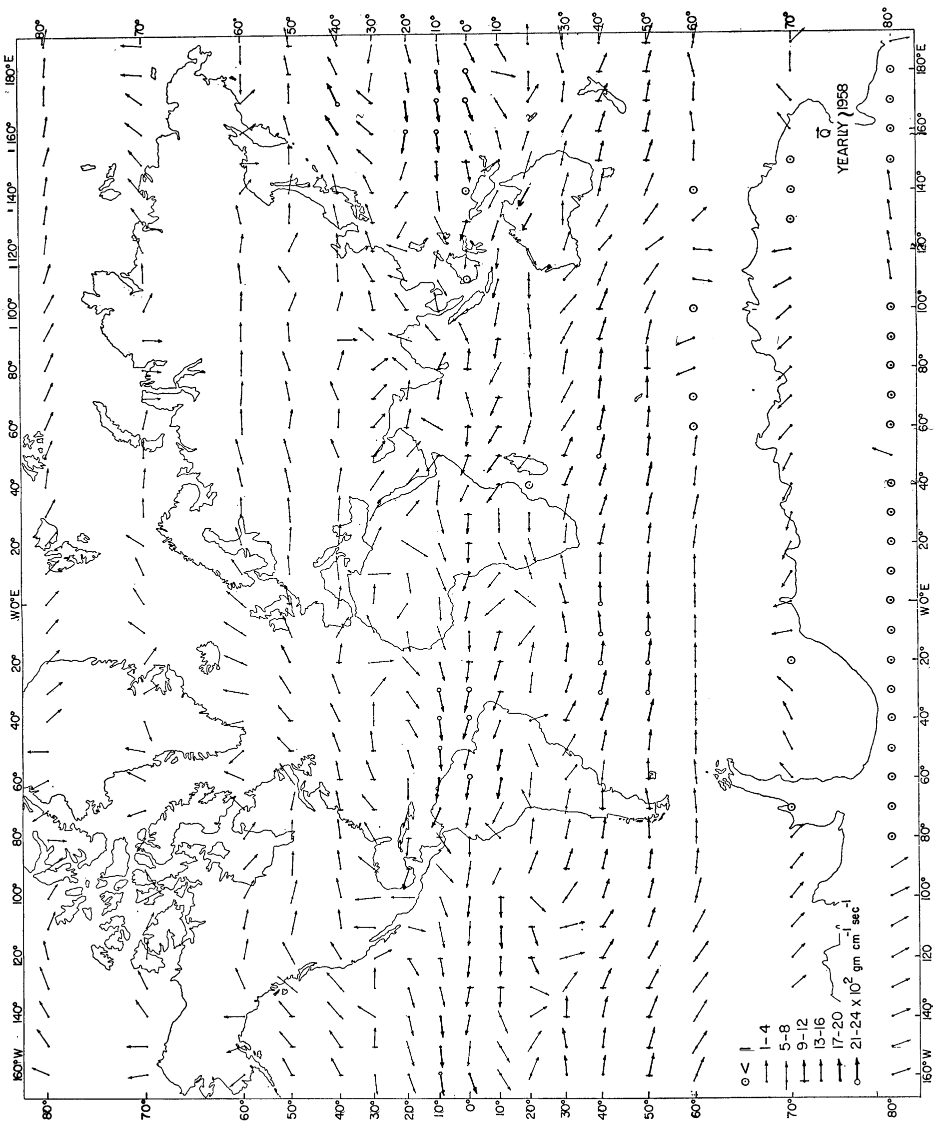

Fig. 6.

Map showing the distribution of the net water vapor transport vector $\overline{\overrightarrow{Q}}(\lambda,\Phi)$ averaged for the IGY, calendar year 1958.

$$Q_{\Phi} = \frac{1}{g}\int_{p}^{p_o} qv\,dp$$

where u and v are the zonal and meridional components of the wind field. This map gives the general description of the main features of the mean total transport of water vapor in the atmosphere.

The transfer is predominantly zonal ($\overline{Q}_{\lambda} > \overline{Q}_{\Phi}$) with midlatitude westerly transports alternating with low latitude easterlies. On the average the change from eastward to westward transport occurs around 25°N and 22°S. Two westerly moisture jets are found in the vicinity of 45° latitude in both hemispheres. In the intertropical belt the flow of moisture is mainly from the East. However, the $\overline{\vec{Q}}$ field is not uniform in intensity and direction. The intensity is largest over the ocean areas (e.g., Pacific, Atlantic, South Indian Ocean). The analysis reflects the main characteristics of the general circulation in the lower part of the atmosphere, as expected. However, inspection shows that, in general, there is a transfer of water vapor from the oceans into the continents. Even when the vectors are mainly zonal, their intensities over the oceans are larger by far than over the continents so that a net inland flow of water results. In some cases this inland transfer is evident from the vector direction (e.g., Gulf of Mexico, etc.). The nonuniformity of the $\overline{\vec{Q}}$ field distribution leads immediately to the impossibility of accepting the evaporation-precipitation *in situ* theory.

Although the zonal component exceeds in general the meridional component, the $\overline{\vec{Q}}$ field is far from being truly zonal. Large asymmetries in the planetary distribution both in intensity and direction are shown. In fact, the analysis of the $\overline{\vec{Q}}$ field shows that there is a net transfer of moisture across the equator from the Southern Hemisphere. The $\overline{Q}_{\Phi}$ component in certain respects is far more important for the water balance of the globe than the $\overline{Q}_{\lambda}$ component.

To illustrate in a concise form the main characteristics of the mean meridional flux and its importance for the water budget of the earth, meridional profiles of longitudinally averaged values $[\overline{Q}_{\Phi}]$ for yearly and seasonal conditions are shown in Fig. 7. The inspection of the yearly profile shows that the largest northward transports (positive values) occur around middle latitudes (40°N) in the Northern Hemisphere and the subequatorial belt (5°S) in the Southern Hemisphere. The most intense southward flux (negative values) occur in the subequatorial belt in the Northern Hemisphere (10°N) and in the middle latitudes (40°S) in the Southern Hemisphere. As the $[\overline{Q}_{\Phi}]$ profile shows, there is a considerable amount of water vapor flux across the equator from the Southern Hemisphere, which feeds the required moisture to the intertropical convergence zone, which on the average is found to the north of the equa-

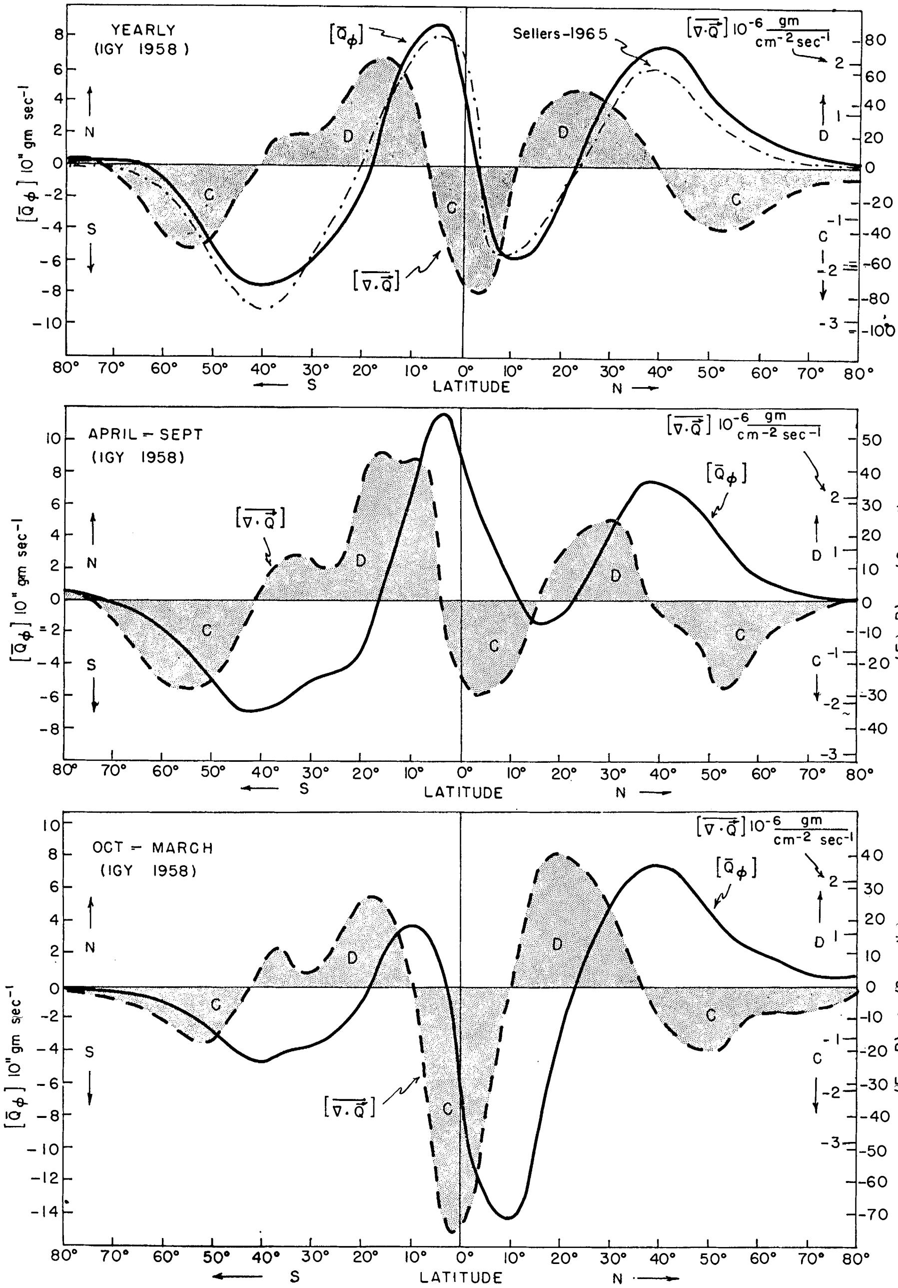

Fig. 7.

Meridional profile of the zonally averaged total water vapor transport $[\overline{Q}\,(\Phi)]$ across latitudinal walls in the atmosphere for the IGY mean yearly and seasonal conditions in units of 10^{11} gm sec^{-1} (scale on left). The thin dashed curve represents the meridional transport of water in the atmosphere for balance as quoted by Sellers. The panel includes also the corresponding distributions of mean zonal divergence of water vapor flux $[\overline{\nabla \cdot \vec{Q}}]$ (heavy dashed curves) in units of 10^{-6} gm cm^{-2} sec^{-1} and in terms of $\overline{[E-P]}$ in cm per year and cm per 6 months (scales on right).

tor. As mentioned before, the evaporation exceeds the precipitation in subtropical latitudes, whereas the reverse conditions prevail in middle and higher latitudes and in the equatorial zone. Thus, the general circulation of the atmosphere must adjust itself so that the motions are such as to transport water from the subtropical regions in both hemispheres to lower and also to higher latitudes. The cycle is closed by a compensating return transport resulting from the combined effects of ocean currents, rivers and underground flow. From the excess of precipitation over evaporation computed from climatological data, Sellers (1965) estimated the required meridional transport of water by the atmosphere. The resulting curve is also shown in Fig. 7. The agreement with the $[\overline{Q_\Phi}]$ profile obtained by the aerological method for the IGY data appears to be excellent.

When seasonal profiles are compared, some striking differences appear in the positions and intensities of the extremes of the meridional water flux. In the April–September profile the largest positive values (northward) occur in the neighborhood of 38°N and 5°S, whereas the maximum southward transports are shown around 15°N and with a much stronger intensity around 40°S. The October–March curve shows a maximum northward transport in the vicinity of 40°N and 10°S, the last being much less intense now. Strong southward transport occurs around 10°N and in middle latitude regions of the Southern Hemisphere. In comparing the two $[\overline{Q_\Phi}]$ curves the conditions are almost reversed when the Northern Hemisphere data are compared with the corresponding values of the Southern Hemisphere. An interesting feature exhibited is the seasonal reversal of the direction of the net flux across the equator, northward and much stronger in the April–September semester ("warm season" of the Northern Hemisphere) and southward, although not as strong, in the October–March semester ("warm season" of the Southern Hemisphere). This unbalanced transport associated with the shift in latitude of the maximum northward and southward transports is a reflection of the monsoon effects and the well-known shifting toward the north of the intertropical convergence zone during the "warm season" of the Northern Hemisphere.

THE DIVERGENCE FIELD

The maintenance of the mean water vapor distribution in the atmosphere against losses due to precipitation and gains due to evaporation requires some mechanism which can compensate for the lack of balance over a given region created by the mean difference between evaporation and precipitation. The balance requirement is accomplished by the divergence field of the total water vapor transport, as has been discussed previously (Peixoto 1970b). Since the mean annual conditions were already discussed in this reference, we shall present here in Figs. 8 and 9 the two-dimensional field analysis of the mean seasonal divergence of the total vertically integrated water vapor transport, $\overline{\nabla \cdot \vec{Q}}$. As we know, the mean rate of change of precipitable water for a given region $\overline{\frac{\delta W}{\delta t}}$ in the atmosphere for the whole year is in general much smaller than $< \overline{\nabla \cdot \vec{Q}} >$. Here the $< (\ ) >$ brackets designate the areal average over a region. Thus for all practical purposes, taking the time average for the period of one year, the equation for water vapor balance

$$< \overline{\frac{\delta W}{\delta t}} > + < \nabla \cdot \overline{\vec{Q}} > = < \overline{E - P} >$$

becomes

$$< \frac{1}{\alpha \cos \Phi} \left[\frac{\delta \overline{Q} \lambda}{\delta \lambda} + \frac{\delta}{\delta \Phi} (\overline{Q}_{\Phi} \mathrm{Cos} \Phi) \right] > = < \overline{E - P} >$$

where α denotes the mean radius of the earth.

For details and general comments on the formulation see Peixoto 1970a. Positive values of divergence show areas where the total evaporation E exceeds the precipitation P, while negative values are associated with regions where total precipitation surpasses the evaporation.

The analyses show considerable detail and, as discussed in the reference above, the most prominent features of the analysis of the divergence flux are closely related to the physiography and the hydrology of many regions on the earth's surface. In both semester maps, areas of convergence are located over the headwaters and drainage basins of large river systems. On the other hand, divergence centers are noted over arid regions. Convergence prevails mostly over the equatorial and middle to high latitude regions, while divergence predominates over the subtropical regions. The middle to high latitude convergence regions in both hemispheres are associated with the behavior of the polar fronts, with the cyclogenetic activity much more intense during the corresponding "cold season" in each hemisphere. The equatorial convergence centers are associated with the activity of the intertropical zone and the moisture convergence is due to the transport accomplished by the lower branch of the Hadley cell towards the region of mean rising motion, where it condenses, leading to heavy precipitation. The seasonal shifting of the equatorial maximum convergence from just south of the equator in October–March to just north in April–September is the consequence of the condensation accompanying the rising branches of the mean Hadley cells that shift northward with the displacement of the sun.

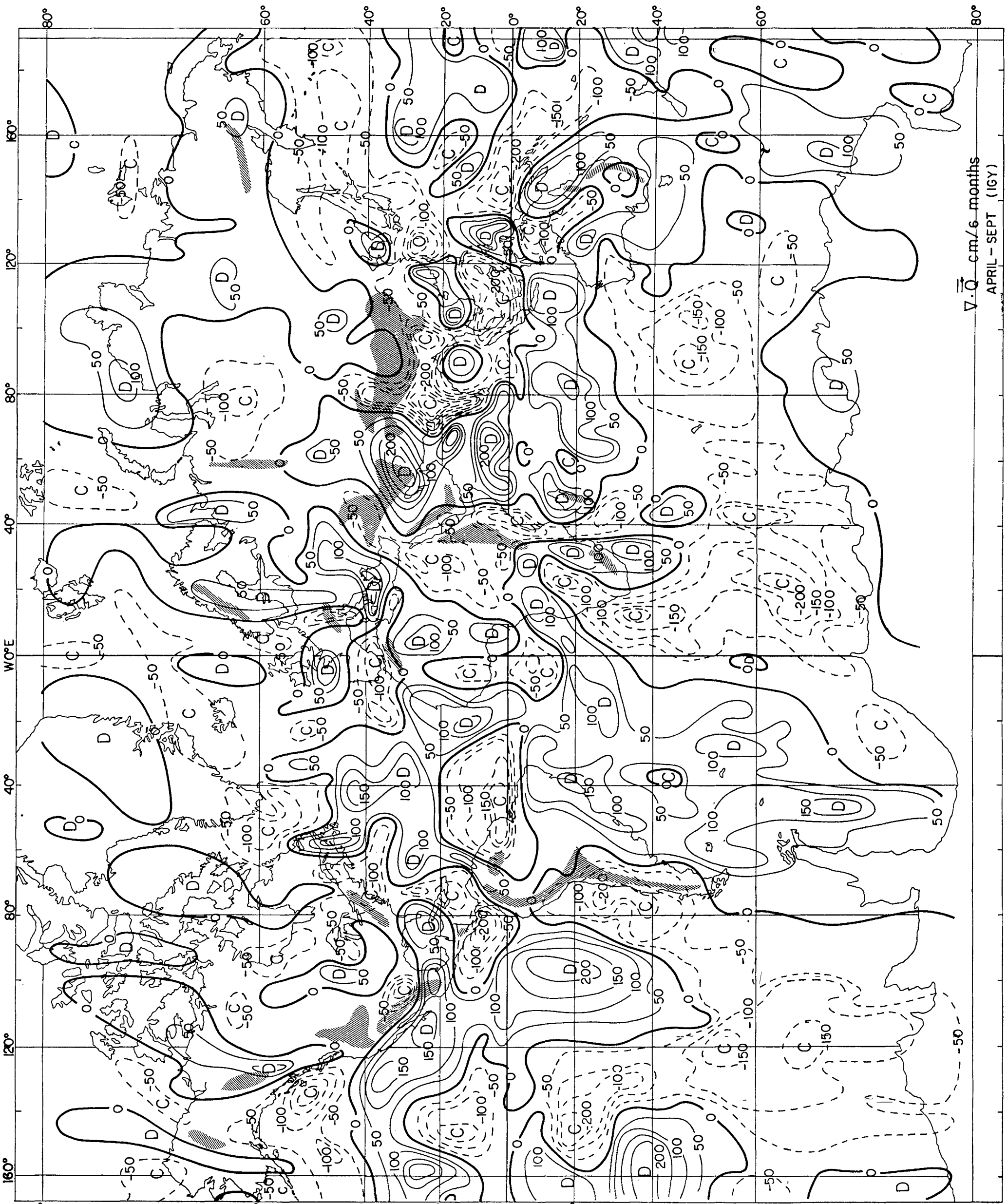

Fig. 8.
Map showing the distribution of the horizontal divergence of the vertically integrated total flux of water vapor, $\nabla \cdot \vec{Q}\,(\lambda,\Phi)$, for the IGY April–September semester in gm per cm^2 per semester. The isopleths (full lines for divergences and dashed lines for convergence) are entered for intervals of 50 gm cm^{-2} $semester^{-1}$.

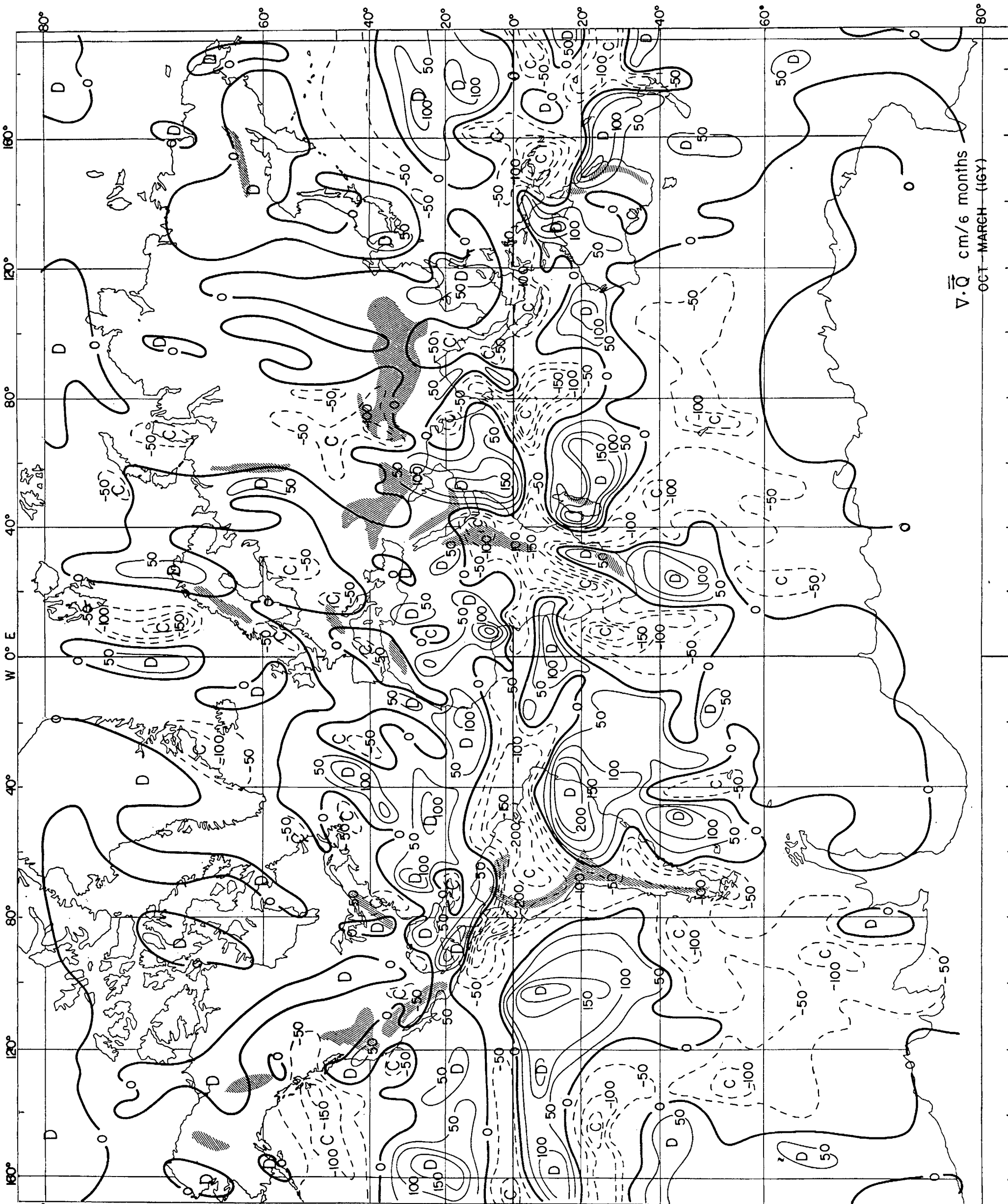

Fig. 9.

Map showing the distribution of the horizontal divergence of the vertically integrated total flux of water vapor, $\nabla \cdot \overline{\overline{\vec{Q}}}(\lambda,\Phi)$, for the IGY October–March semester in gm per cm^2 per semester. The isopleths (full lines for divergences and dashed lines for convergence) are entered for intervals of 50 gm cm^{-2} $semester^{-1}$.

Divergence over the subtropical latitudes is more intense during the "cold season" of each hemisphere and occurs mainly over regions where anticyclones are predominant. Strong subsidence leads to cloud-free dry air which favors the evaporation. The shifting of the maximum belt of divergence accompanies the mean yearly movement of the anticyclones in both hemispheres which generally recede polewards from the "cold" to the "warm season".

Over the Northern Hemisphere the actual analyses for the seasons agree with those published by the writer (1959). Over the Southern Hemisphere they are consistent with the study of Taljaard (1967) on the development, distribution and movement of cyclones and anticyclones during the IGY, and they also agree with the general characteristics of the atmospheric circulation during the same period as discussed by van Loon (1965, 1967). Over the north polar regions there are indications that divergence predominates in the mean, while over the border of Antarctica at least, convergence seems to be the dominant condition.

When areas of divergence (i.e., in which $(\overline{E-P}) > o$) occur over ocean surfaces, there is no difficulty concerning the necessary supply of water for evaporation. However, when they occur over land, as for example over the arid regions, the situation is completely different. It must be the surface and underground flow from less arid regions which supplies the required water that accounts for the observed excess of evaporation. The study of the hydrology of deserts is an extensive and difficult subject, although of paramount importance and great practical value. This aspect has been treated previously (for details consult Starr & Peixoto 1958, Peixoto 1960, 1970a, 1970b).

Over the oceans the interpretation of the divergence field is easier due to the nature of the underlying surface. It is no longer necessary to speculate on the nature and magnitude on the compensating flow for a given divergence field feature, because the oceans, being fluid, find the necessary motion to adjust and to maintain equilibrium. There are both convergence and divergence centers over the oceans and they are more intense than over the continents. Divergence is associated with the subtropical anticyclones in both hemispheres. These regions constitute the major source of the atmospheric moisture. Since over these regions evaporation exceeds by far the precipitation, an increase in salinity is to be found under divergence centers, and since the opposite would be true in a region of convergence, the addition of fresh water would lead to a dilution and so to lower values of salinity. A comparison of the actual analysis of the divergence flux with salinity distribution charts over the oceans reveals that there is a close relationship between the main features of both distributions. Thus, a good correlation exists between the hemispheric oceanic divergence values and the corresponding salinity values (Peixoto 1959, Lufkin 1959). This approach has proved to be worthwhile in oceanography studies (von Arx 1962).

It should however be pointed out that the maps presented in Figs. 8 and 9 give a too detailed picture of the divergence field considering the method used and the lack of data over some regions.

For example the maps do not agree for some areas with well-known facts concerning evaporation and precipitation.

MEAN PLANETARY WATER BALANCE AND THE GENERAL CIRCULATION OF THE ATMOSPHERE

The general circulation of the atmosphere must include a complete description of the global distribution of atmospheric properties, considering not only spatial and temporal mean conditions but also higher moments of the probability distribution through a complete set of statistics. It then comprises more than the time averaged state of the atmosphere with all of its geographical features, and more than a global description of the permanent and semi-permanent synoptic centers of action of the atmospheric circulation. Hence the necessity of evaluating, among other things, the eddy moisture transport fields to give a better view of the global atmospheric vapor distribution and motion in connection with the general circulation. One such study of the eddy flux of moisture from pole to pole has already been accomplished and will be published elsewhere (Starr & Peixoto 1971).

However, at this point it seems appropriate to show how we can use the mean values of the divergence field to infer some climatological implications and how these consequences are associated with some features of the general circulation taken *in sensu lato*. For a latitudinal belt bounded by the latitude Φ_1 and Φ_2 the mean zonal divergence of the water vapor can be evaluated from the mean total meridional transport of water vapor, $\overline{Q}_\Phi$, using the expression

$$[\nabla \cdot \overline{\vec{Q}}] \approx [\overline{E-P}] = \frac{1}{2\,\pi\,(\sin \Phi_2 - \sin \Phi_1)}\, \varphi\, [(\overline{Q}_\Phi \cos \Phi)_{\Phi 2} - (\overline{Q}_\Phi \cos \Phi)_{\Phi 1}]\, d\lambda$$

These values can be compared with the corresponding climatological estimates of $[\overline{E-P}]$, since it can be assumed that for long periods of time $\overline{\frac{\delta W}{\delta t}} = o$.

Actually the mean values of divergence by 5° latitude belts were computed and the corresponding profiles are shown in Fig. 7. These profiles synthesize the main features of the two-dimensional distribution of $\nabla \cdot \overline{\vec{Q}}$ fields as given in Figs. 8 and 9.

The $[\nabla \cdot \overline{\overline{\vec{Q}}}]$ profiles in Fig. 7 show in all the cases strong convergence of water vapor with an excess of precipitation over evaporation ($[\overline{E-P}] < 0$), over the equatorial region, which is accomplished by the trade winds in both hemispheres and is responsible for the observed heavy precipitation. Other convergence zones shown in middle to high latitude regions are due to the circulations associated with the transient cyclones which travel along the polar fronts and to the semi-permanent features of the circulation in high latitudes of both hemispheres.

Divergence ($[\overline{E-P}] > o$) is found in subtropical latitudes and as mentioned is associated with the large anticylonic circulations which prevail over these regions in the Northern and in the Southern Hemispheres. There seems to be a divergence in the northern subpolar region, and some convergence in the rim of Antarctica. The subtropical regions act as the primary sources of moisture for the atmosphere, while the equatorial and middle latitude regions act as sinks.

Numerical estimates of $[\nabla \cdot \overline{\overline{\vec{Q}}}] \approx [\overline{E-P}]$ for 10° latitude belts are shown in Table 2, together with corresponding independent estimates of $[\overline{E-P}]$ from previous aerological studies and from climatological normals, as quoted by Sellers (1965). Table 2 shows a good agreement on the whole between various sets of values of $[\overline{E-P}]$, except for some differences which are explained by the fact that these computations are for one year only and thus are not directly comparable with climatological data taken from normals. However, it seems that on the whole zonally averaged values of $[\nabla \cdot \overline{\overline{\vec{Q}}}]$ are quite satisfactory. It appears that the aerological method may give more reliable values especially over large oceanic areas than the conventional hydrological methods. The current type of approach is of great importance not only for the study of the global energetics of the earth's atmosphere as is obvious, but also in other fields, namely oceanography and in the modern developments of hydrology (see Eagleson 1969). In theory, at least, the integrated total water vapor transport can be used to evaluate the net inflow (convergence) or outflow (divergence) of water vapor for a given region during a certain period of time. However, in practice several difficulties arise as has been shown by several authors (Hutchings 1957, Peixoto 1959, Rasmusson 1967, etc.). At the present time the aerological approach can be used successfully only in regions of large area with a relatively dense network of aerological stations for periods of at least a few days (Rasmusson 1967, Peixoto 1970).

A superficial analysis of the $[\overline{\overline{Q}}_\Phi]$ and of the $[\nabla \cdot \overline{\overline{\vec{Q}}}]$ profiles leads to the conclusion by indirect evidence of the existence of two three-cell regimes with two direct cells (Hadley and polar cells) and one indirect cell (Ferrel cell). It is also true that in low latitudes the contribution of the Hadley cell for the

Table 2.

Distribution of zonally averaged mean divergence of water vapor flux, $[\overline{\nabla \cdot \vec{Q}}]$ derived from present study. These results are compared with mean differences between precipitation and evaporation, $[\overline{E-P}]$, as derived from independent previous estimates by other investigators using aerological data and climatological normals. All units are in cm year^{-1}.

	0–10°	10–20°	20–30°	30–40°	40–50°	50–60°	60–70°	70–80°
				Northern Hemisphere				
Present study, $[\overline{\nabla \cdot \vec{Q}}]$	–75.34	30.25	48.37	25.50	–26.55	–36.37	–19.19	–10.44
Budyko (Sellers)	–69.90	23.80	45.60	13.00	–26.60	–32.00	– 8.30	– 5.00 (70–90°)
Starr and Peixoto	–43.30	25.10	43.30	21.80	– 1.40	–36.10	–30.10	–17.30
Peixoto and Crisi	–42.50	30.30	48.50	26.60	–26.00	–36.20	–19.20	– 8.30 (70–90°)
Conrad and Wüst	–43	37	48	19	–32	–32	–25	–22
				Southern Hemisphere				
Present study, $[\overline{\nabla \cdot \vec{Q}}]$	–19.28	66.34	27.87	18.16	–19.39	–52.32	–22.06	4.12
Budyko (Sellers)	–14.10	40.90	55.90	32.40	–33.10	–52.60	–24.40	– 3.70

total equatorward transport of water vapor becomes dominant, whereas the contributions of the other two cells account for only a small fraction of the total meridional flux of water vapor, the eddies being by far the more important factor in the total process (see Starr & Peixoto 1971). In fact, in transporting water vapor both the transient and standing eddies act opposite to the total flux in the equatorial regions. They can be regarded as a mechanism that takes away the excess of moisture transported into the equatorial region by the Hadley cells. However, in middle and high latitudes eddies are the most important mechanism for the total convergence observed in those regions. They act in this case as the vehicle for the meridional poleward accumulation of the excess of water vapor produced in the subtropical anticyclonic sources where strong divergence predominates.

The excellent agreement of the actual results with those obtained in previous studies seems to secure the consistency of the approach followed and of the methodology utilized. Therefore it seems reasonable to expect that in extending to the Southern Hemisphere the same methodology, the results obtained will depict the most prominant characteristics of the flow of the water vapor. However, with the necessary improvement of the Southern Hemispheric network and the implementation of new instrumental techniques, much can be done to improve the actual results. It is anticipated that a similar study using five years of data on a global scale will be produced in the near future.

ACKNOWLEDGMENTS

The writer wishes to express his appreciation for the support provided by the U.S. National Science Foundation under Grant No. GA-1310X. Also, the writer wishes to thank Professor Victor P. Starr for his most valuable suggestions, discussions and advice given during the preparation of this paper. Thanks are also due to Mrs. Rachel Morton for programming help.

REFERENCES

Eagleson, P. S. (1970) *Dynamic hydrology.* McGraw-Hill, New York, 462 pp.

Hutchings, J. W. (1961) Water-vapor transfer over the Australian continent. *J. Meteorol. 18,* 615–634.

Lufkin, D. (1959) Atmospheric water divergence and the water balance at the earth's surface. Sci. Rep. No. 4, General Circulation Project, M.I.T.

Peixoto, J. P. (1959) O campo da divergencia do vapor de agua na atmosfera. *Rev. Fac. Cien. Lisboa,* 2a, Ser. VII, 25–56.

Peixoto, J. P. (1960) On the global water vapor balance and the hydrological cycle. *Tropical meteorology in Africa.* Munitalp Foundation, Nairobi, Kenya, 232–243.

Peixoto, J. P. (1970) Water vapor balance of the atmosphere from five years of hemispheric data. *Nordic Hydrology 2,* 128–138.

Peixoto, J. P. (1970b) Pole-to-pole divergence of water vapor. *Tellus 22,* 17–25.

Peixoto, J. P. (1971) Atmospheric vapor flux computations for hydrological purposes. Proceedings of RA-VI Working Group on Hydrology, W.M.O. held in Geneva, Feb. 15–19, 1971. (In press).

Peixoto, J. P. & Crisi, A. R. (1965) Hemispheric humidity conditions during the IGY. Sci. Rep. No. 6, Planetary Circulations Project, M.I.T.

Peixoto, J. P. & Obasi, G. O. P. (1965) Humidity conditions over Africa during the IGY. Sci. Rep. No. 7, Planetary Circulations Project, M.I.T.

Rasmusson, E. M. (1967) Atmospheric water vapor transport and the water balance of North America. *Monthly Wea. Rev. 95,* 403–425.

Sellers, W. D. (1965) *Physical climatology.* University of Chicago Press, Chicago, 272 pp.

Starr, V. P., Peixoto, J. P. & McKean, R. (1968) Pole to pole moisture conditions for the IGY. *Pure and Appl. Geoph. 15,* 300–331.

Starr, V. P. & Peixoto, J. P. (1971) Pole-to-pole eddy transport of water vapor in the atmosphere during the IGY. Arch. f. Meteor., Geoph. u. Biokl. (In press).

Taljaard, J. J. (1967) Development, distribution and movement of cyclones and anticyclones in the southern hemisphere during the IGY. *J. Appl. Meteor. 6,* 973–987.

van Arx, W. S. (1962) *An introduction to physical oceanography.* Addison-Wesley Publ. Co., Reading, Massachusetts, 422 pp.

van Loon, H. (1965) A climatological study of the atmospheric circulation in the southern hemisphere during the IGY, Part I. *J. Appl. Meteorol. 4,* 479–491.

van Loon, H. (1967) A climatological study of the atmospheric circulation in the southern hemisphere during the IGY, Part II. *J. Appl. Meteorol. 6,* 803–815.

Address:

Prof. José P. Peixoto, M.I.T., Department of Meteorology,
Room 54–1522, Cambridge, Massachusetts 02139, USA.

Received 1 October 1971.